Macromolecules

ARTICLE

pubs.acs.org/Macromolecules

Equilibrium Chain Exchange Kinetics of Diblock Copolymer Micelles: Effect of Morphology

Reidar Lund,[*,†,‡] Lutz Willner,[*,§] Vitaliy Pipich,[⊥] Isabelle Grillo,[∥] Peter Lindner,[∥] Juan Colmenero,[†,‡] and Dieter Richter[§]

[†]Donostia International Physics Center, Paseo Manuel de Lardizabal 4, 20018 Donostia—San Sebastián, Spain

[‡]Centro de Física de Materiales, Centro Mixto CSIC-UPV/EHU, Paseo Manuel de Lardizabal, 3, 20018 Donostia—San Sebastián, Spain

[§]Jülich Centre for Neutron Science JCNS and Institute for Complex Systems ICS, Forschungszentrum Jülich GmbH, 52425 Jülich, Germany

[⊥]Jülich Center for Neutron Science JCNS-FRM II, Forschungszentrum Jülich GmbH, 52425 Jülich, Germany

[∥]Institut Laue-Langevin, F-38042 Grenoble, France

ABSTRACT: In this work, we present the chain exchange kinetics in block copolymer micelles of spherical and cylindrical geometry. The aim of this work was to understand the mechanisms controlling the molecular exchange with a particular focus to delineate any potential effect of the micellar morphology. As model system symmetric short-chain amphiphilic poly(ethylene-*alt*-propylene)-poly(ethylene oxide) diblock copolymer (PEP1−PEO1, numbers denote approximate molecular weight in kD) in aqueous solutions has been used. This system undergoes a irreversible cylinder to sphere transition upon addition of *N*,*N*-dimethylformamide (DMF) as cosolvent or upon heating. This feature allowed to quantitatively compare chain exchange kinetics in both morphologies. The kinetics were accessed by using hydrogen/deuterium labeling and time-resolved small-angle neutron scattering experiments employing a stopped flow apparatus by which the kinetics could be followed from about some hundreds of milliseconds up to hours. The results show that, independent of morphology, all data can be satisfactorily described by a scaling model that takes into account the polydispersity of the core forming PEP block in order to describe the broad logarithmic time decay at longer times. A small but significant effect of the morphology could be seen which was reflected in a slightly accelerated kinetics for spherical micelles. A detailed comparison shows that for both morphologies, the activation energy follows a scaling law proportional to the product of the interfacial tension, γ, and the number of repeat units of the insoluble block, N_B, i.e., $E_a \sim \gamma N_B$ rather than the $\gamma N_B^{2/3}$ predicted by Halperin and Alexander. This implies a stretched conformation of the insoluble block during the expulsion process compared to the more globular shape considered in the original scaling theory. This can be related to insufficient chain length/statistics for these rather small chains to form a globule during the expulsion process; or to an higher polymer density within the corona of these "crew cut" type micelles. Through the analysis, the faster kinetics could be summarized in a slightly smaller activation energy for the spherical micelles which is probably related to small changes in the internal corona structure.

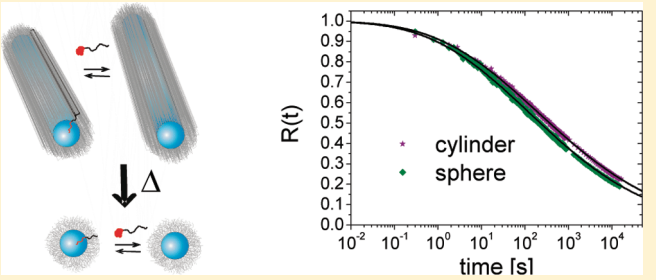

1. INTRODUCTION

Micelles are usually assumed to be in dynamic equilibrium where the constituting molecules are continuously redistributed among the micellar entities due to stochastic thermal fluctuations.[1,2] This is a consequence of the closed association concept where the micellar aggregation number fluctuates around its mean value representing the global free energy minimum. The equilibrium kinetics of low molecular weight surfactant micelles have been studied extensively during the 1970−1980s.[3] Anniansson and Wall have discussed theoretically and later shown experimentally that the exchange mechanism is dominated by the exchange of individual surfactant molecules.[4−6] For block copolymer micelles on the other hand the equilibrium kinetics has been by far less understood. On the basis of the Aniansson and Wall mechanism the chain exchange was calculated theoretically by Halperin and Alexander[7,8] using scaling analysis. Accordingly, the characteristic relaxation function should follow a single exponential decay as it is expected for "reaction limited" exchange kinetics governed by unimer expulsion. However, as was shown recently by time-resolved small angle neutron scattering experiments (TR-SANS) the characteristic relaxation function describing the fraction of chains that are exchanged almost perfectly follows an extremely broad close to logarithmic decay over several decades in time.[10−12] This phenomenon was observed independently in several block copolymer/solvent systems and is also consistent with earlier observations of a

Received: March 8, 2011
Revised: June 30, 2011
Published: July 15, 2011

broad relaxation seen by other techniques,[13−15] where such behavior sometimes was related to several mechanisms.[14] An attempt to describe the data by taking into account the finite polydispersity of the polymer chains was presented in refs 10 and 11. In the latter work it was shown that by using the theory of Halperin and Alexander and a suitable chain length distribution (Poisson distribution), a poor description of the data was obtained. As a different approach the observed logarithmic decay was assigned to constrained polymer dynamics within the micellar cores. In fact such confinement induced polymer dynamics have been proposed from theory and nuclear magnetic resonance (NMR) experiments.[23] However, experiments by neutron spin−echo (NSE) spectroscopy on polymers in confined geometries,[19−21] did not reveal any particular "constrained" dynamics. Hence, the reason for the logarithmic decay would have to be sought elsewhere.

Indeed very recently, Choi, Lodge, and Bates[16] suggested from data on poly(styrene)−poly(ethylene-*co*-propylene) (PS−PEP) block copolymers in squalane that the logarithmic exchange kinetics can be explained by the polydispersity of the core forming block alone. This was assigned to the hypersensitivity of the chain length on the kinetics due to a double exponential dependence. In principle virtually the same polydispersity model for unimer exchange that was introduced by some of us[10,11] was employed, however, they allowed for a free prefactor that scales with the activation energy. In addition they considered a stronger dependence on the degree of polymerization of the core block, N_B, on the activation energy, E_a, which scales linearly with N_B implying a completely stretched chain or a θ-like chain instead of $E_a \sim N_B^{2/3}$ which would corresponds to a collapsed coil conformation during the expulsion process. Finally they introduced the Rouse time $\tau_R \sim N_B^2$ of the homopolymer melt in question as a pre-exponential factor.

In light of these results some of us have reanalyzed the kinetic data from amphiphilic poly(ethylene-*alt* propylene)−poly(ethylene oxide) (PEP−PEO) block copolymer micelles by introducing the temperature dependent prefactors into the original model.[10,11] Now an almost perfect description of the data was possible, but differently from the results of Choi et al.,[16] $E_a \sim N_B^{2/3}$ could fit the data.[17] Although by now the logarithmic decay seems to be sufficiently explained by the polydispersity of the core block, there still remain open questions concerning the polymer conformation in the activated steps of the exchange process. Moreover, so far all experiments have been performed in micelles with spherical symmetry and no evaluation of the potential influence of the micellar morphology has been presented.

In the present work we focus on the molecular exchange kinetics in block copolymer micelles of spherical and cylindrical morphology. The micelles are formed by a short chain poly(ethylene-*alt*-propylene)-poly(ethylene oxide) block copolymer (PEP1−PEO1, with 1 as the approximate molecular weight in kD), in various *N*,*N*-dimethylformamide/water mixtures as selective solvent. Variation in the solvent composition affects both kinetic and structural properties of the micelles via changes of the interfacial energy. As in prevous work,[10,11] DMF cosolvent addition was used to tune the kinetic rate which for this system is essentially frozen in pure water (high interfacial tension, γ) and fast in DMF-rich solutions (low γ). Moreover, in a preceding structural study we have shown that the PEP1−PEO1 block copolymer forms cylindrical micelles in water-rich solutions while at about 50 mol % DMF the cylindrical micelles spontaneously transform into spherical geometry. At intermediate DMF concentrations, this transition can also be induced irreversibly by temperature. Hence by using the same PEP1−PEO1 polymer we were able to study the molecular exchange in the different geometries just by variation of the DMF/water ratio and thereby scrutinize any potential effect of the morphology. As the PEP1−PEO1 block copolymer forms "crew-cut" type micelles, it is further interesting to compare it with the "starlike" micellar structure of the PEP1−PEO20/water/DMF system investigated before. The kinetics have been measured by TR-SANS experiments using a sophisticated H/D labeling technique as already described in detail in previous publications.[9−11] The experiments were performed at DMF/water compositions close to the morphological transition at 41 and 47 mol % DMF for the cylinders and 60 and 75 mol % DMF for the spheres. At 51 mol % DMF, kinetics have been measured before and after the thermally induced cylinder to sphere transition which thereby allowed the kinetics to be compared directly of exactly the same system in two different morphologies without changing any other parameters. In order to obtain a broad dynamic range from about 100 ms to several hours we have applied high-flux SANS coupled with a stopped-flow apparatus for fast and reproducible mixing.

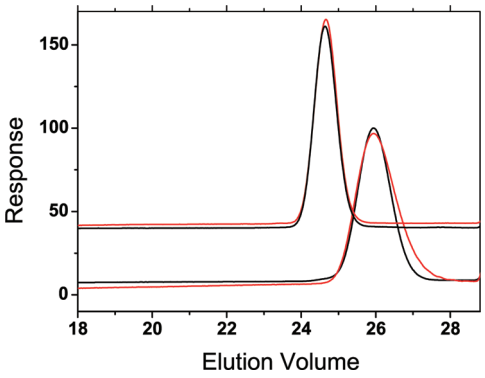

Figure 1. SEC curves of d-PEP1−d-PEO1 (red) and h-PEP1−h-PEO1 (black) and the corresponding PEP-precursors in THF/DMA 85/15 at 40 °C.

2. EXPERIMENTAL SECTION

2.1. Materials. *2.1.1. Polymer Synthesis and Characterization.* The h-PEP1−h-PEO1 (hh) polymer is identical with the one used in the structural study published previously.[24] The synthesis and characterization has already been described there. For the chain exchange kinetics, which is subject of this paper, a fully deuterated analogue d-PEP1−d-PEO1 (dd) was prepared accordingly by anionic polymerization. We followed essentially the two step procedure described in detail in an earlier publication.[25] As monomers perdeuterated isoprene (>98% D) (Cambridge Isotope Laboratories) and ethylene oxide (>98% D) (Eurisotop) were used. The synthesis involved the preparation of a OH-terminated d-polyisoprene precursor block which subsequently was saturated with deuterium to the corresponding d-PEP1−OD polymer. The d-PEP1−OD polymer was transferred to a macroinitiator with potassium as counterion serving as initiator for the polymerization of the deuterated ethylene oxide. The resulting dd-polymer was characterized by size exclusion chromatography (SEC) in tetrahydrofuran/dimethylacetamid (85/15) as eluent at 40 °C. Figure 1 shows the chromatograms of the d-PEP1−OD precursor and the d-PEP1−d-PEO1 block copolymers together with those of the corresponding h-PEP1−OH and h-PEP1−h-PEO1 polymers. It becomes apparent that both the PEP precursors and the PEP−PEO block copolymers have

Table 1. Molecular Weight Characteristics of PEP1−PEO1 Block Copolymers

	M_n (PEP) (kg/mol)	M_w/M_n (PEP)	N(PEP)	M_n(PEO) (kg/mol)	N(PEO)	M_w/M_n (PEP−PEO)
hh	1200	1.06	17	1500	34	1.04
dd	1400	1.08	17	1600	34	1.04

almost identical elution volumes indicating the same degree of polymerization, N. For the h-PEP and h-PEO block N(PEP) = 17 and N(PEO) = 34, respectively, as determined by ^{1}H NMR. Accordingly, the number-average molecular weight, M_n, of the d-PEP is calculated to be 1400 g/mol and of the d-PEO blocks 1600 g/mol. The SEC curves further reveal an almost identical polydispersity for the block copolymers, while a slightly broader distribution is observed for the d-PEP1-OD compared to the h-PEP1-OH. Using a polystyrene calibration curve the polydispersity, M_w/M_n, was determined to be 1.08 for the PEP block and 1.04 for the final block copolymer. The polymer characteristics are summarized in Table 1.

2.1.2. Samples and Contrast Conditions. For the contrast calculations the scattering length densities of the individual polymers were taken as already ascertained in ref 18 at 20 °C: $\rho_{h-PEP} = -3.01 \times 10^9$ cm^{-2}, $\rho_{h-PEO} = 6.35 \times 10^9$cm^{-2}, $\rho_{d-PEP} = 7.17 \times 10^{10}$ cm^{-2}, $\rho_{d-PEO} = 7.02 \times 10^{10}$cm^{-2}. For the calculation of ρ_{h-PEO}, we have used the bulk density of h-PEO:[30] $d_{h-PEO} = 1.125$ g/cm^3. An attempt to use the reported solution density in water of 1.2 g/cm^3[31] did not influence the results in any significant way as the contrast between the micelles and the deuterated solvent mixtures is in all cases very large. Accordingly, for the d-PEO the bulk density of $d_{d-PEO} = 1.227$ g/cm^3 was taken. By taking into account the block copolymer compositions given in Table 1 and the above-defined scattering length densities the mean values for ρ were calculated to be $\rho_{hh} = 1.47 \times 10^9$ cm^{-2} and $\rho_{dd} = 7.05 \times 10^{10}$ cm^{-2}. Hence $\rho_{average}$ of a blend with $\phi_{hh} = \phi_{dd} = 0.5$ is 3.6×10^{10}cm^{-2}. For the kinetic study isotopic solvent mixtures of D_2O (Armar AG Switzerland 99.8% D), H_2O (Millipore quality), DMF (Aldrich, anhydrous 99.8%) and DMF-d_7 (Chemotrade, Leipzig 99.5% D) were prepared. The solvents were used as received without further purification. All mixtures were composed such that their scattering length densities, ρ_0, matches exactly $\rho_{average}$ of the two block copolymers. ρ_0 was calculated according to

$$\rho_0 = \frac{N_{Avo}\sum_i x_i b_i}{\sum_i x_i M_i} d_{mix} \quad (1)$$

where x_i is the molar fraction of solvent component i and M_i is the molar mass. b_i denotes the sum of the coherent scattering length of all atoms in a solvent molecule and N_{avo} Avogadros number. d_{mix} were individually measured using an Anton Paar DMA 5000 instrument. The DMF mol fractions, X_{DMF}, were 41%, 47%, 51%, 60%, and 75%, respectively. In order to achieve high scattering intensities the structural characterization of the two polymers was performed in full contrast i.e. the protonated block copolymer was measured in d-DMF and D_2O and vice versa. The solutions were made by direct dissolution of the polymer powder in the premixed solvent mixtures to give a final polymer concentration of about 1 vol %. In order to facilitate dissolution of the polymers, the samples were slightly warmed up to 60 °C for approximately 30 min and subsequently equilibrated by shaking overnight at room temperature.

2.2. SANS Experiments and Data Evaluation. The SANS-measurements were carried out using the KWS-2 at the FRM-2 reactor at Garching, Germany, and the D11 instrument at Institut Laue Langevin (ILL), Grenoble, France. The measurements were performed at several sample-to-detector distances and collimation lengths in order to cover an extended Q range and to maintain a reasonable resolution. The wavelengths were set to 7 and 6 Å in Jülich and Grenoble, respectively. At D11 the Q-range was approximately 1×10^{-3} Å$^{-1} \leq Q \leq 0.3$ Å^{-1} and in Jülich 2×10^{-3} Å$^{-1} \leq Q \leq 0.2$ Å^{-1}. Detector sensitivity corrections were made with plexiglass in Jülich while water was used in Grenoble. The same materials were used as secondary standards. Empty cell scattering and the background signal arising from electronic noise, γ radiation and fast unmoderated neutrons were subtracted using standard procedures. The background noise was determined using cadmium (Cd) or boron carbide to block the primary beam. All background subtraction was done directly pixel by pixel on the two- dimensional detector intensity image. After radial averaging the intensities were treated for dead time effects (420 and 650 ns at D11 and KWS2 respectively) in order to yield the absolute normalized macroscopic differential scattering cross sections, $(d\Sigma/d\Omega)(Q)$ in absolute units of cm^{-1}. For more details concerning the calibration/data reduction procedure see, e.g., ref 26.

For rapid mixing, a modified commercial stopped flow apparatus (Biologic, SFM 400 (D11) and SFM 300 (KWS2)) was employed. A special observation cell was set up using a quartz cell (Hellma) with an optical path length of 1 mm. The solutions consisting of the h-PEP1−h-PEO1/DMF/water and d-PEP1−d-PEO1/DMF/water solutions respectively, were injected in a 1:1 proportion into a mixing chamber assuring fast turbulent homogeneous mixing. The mixed solution was then further transported to thicker tubes leading to a smooth laminar flow into the quartz cell which serves as the observation cell for the neutrons. As a reference sample for the kinetics, the initial intensity before any exchange has taken place, $I(t = 0) = I(0)$, needs to be determined. This value was obtained by measuring the reservoirs (hh and dd block copolymers) separately at each DMF compositions before mixing at low concentrations where the structure factor is negligible. The mean value was then used as $I(0)$.

The reservoirs are continuously mixed by injection into the mixing chamber (2 mL/s for both syringes). Afterward the mixed solution is transported into the scattering volume. This mixing and transport takes 50 ms (t_{dead}) and fills the cell. The sampled kinetic times can then be calculated according to $t_i = t_{dead} + t_{i-1} + t_{aq}(i)/2$. The acquisition time, $t_{aq}(i)$, was set to follow a geometric progression in order to improve the statistics and to distribute the data points over a wider time range: $t_{aq}(i) = 200 \times (1.15)^{i-1}$. In order to improve the statistics, the samples were typically mixed and measured 3−5 times and the resulting data combined. In order to study the influence of mixing on the kinetics in one case the two micellar reservoirs were mixed manually. With this method equal volumes of the two reservoirs are transferred with a 1 mL micropipet directly into a standard 1 mm Hellma cuvette. After shaking the cell was fixed into the sample holder before the data collection was started. This method was applied before[10,11,9,12] as a standard procedure but involves a delay time of about 1 min which, therefore, is suitable only for slow kinetics.

The data were treated and corrected using LAMP available at ILL, Grenoble or using the QtiKWS[29] at Garching, Germany.

2.3. SANS Data Modeling and Evaluation of Exchange Kinetics. The scattering models used to analyze the static structural data were either cylindrical or spherical core−shell models as described in a previous publication[24] based on the models by Pedersen et al.[27] In order to take into account effects of experimental smearing in terms of Q, the fit function was convoluted using the approach of Pedersen et al.[28] To obtain quantitative information about the chain exchange kinetics we have applied two methods. The first is model independent and determines the relaxation function $R(t)$[10,11] according to

$$R(t) = \sqrt{\frac{I(t) - I_\infty}{I(0) - I_\infty}} \quad (2)$$

where $I(t) = \int I(Q,t)\, dQ$ is the integral intensity at a given time, I_∞ the intensity of the fully mixed sample at the final stage of the kinetic process (obtained by randomly mixing the two block copolymers with $\phi_{hh} = \phi_{dd} = 0.5$). $I(0)$ was obtained by measuring the normalized intensity of

the reservoirs (hh and dd samples) separately before mixing and performing and arithmetic average.

$I(Q,t) \sim \Delta\rho(t)^2$ where $\Delta\rho(t)$ is proportional to the excess fraction of either h- or d-type block copolymer in the corresponding h- or d-type micelles, $R(t)$ $(0 \le R(t) \le 1)$ is a measure of the amount of block copolymer that has exchanged at least once.[11]

The second method is model dependent and employs a time dependent scattering function which independent of the morphology (spherical or cylindrical) allows to calculate the scattering intensity, $I(Q,t)^i$ as a function of time:

$$\begin{aligned} I(Q,t)^i = {} & \frac{\phi}{PV_{\mathrm{PEP-PEO}}}(\Delta\rho_c^i(t)^2 P^2 \cdot {V_{\mathrm{PEP}}}^2 \cdot A(Q)_c^{\,2} \\ & + \Delta\rho_{sh}^i(t)^2 P \cdot (P - F(0)_{\mathrm{blob}}) \cdot {V_{\mathrm{PEO}}}^2 \cdot A(Q)_{sh}^{\,2} \\ & + 2\Delta\rho_c^i(t) \cdot \Delta\rho_{sh}^i(t) P^2 \cdot V_{\mathrm{PEO}} \cdot V_{\mathrm{PEP}} \cdot A(Q)_c A(Q)_{sh} \\ & + {V_{\mathrm{PEO}}}^2 \Delta\rho_{sh}^i(t)^2 \cdot F_{\mathrm{blob}}(Q)) \end{aligned} \tag{3}$$

Here i denotes either protonated (i = h) or deuterated (i = d) species. $A(Q)$ is the scattering amplitude of core (c) and shell (sh), respectively. The scattering amplitude for the core can be written as

$$A(Q)_c = \begin{cases} \dfrac{3(\sin(Q \cdot R_c) - Q \cdot R_c \cos(Q \cdot R_c))}{(Q \cdot R_c)^3} \cdot \mathrm{DW}(Q,\sigma) & \text{spheres} \\ \dfrac{\sin(Q \cdot L \cos(\alpha)/2)}{Q \cdot L \cos(\alpha)/2} \dfrac{2J_1(Q \cdot R_c \sin(\alpha))}{Q \cdot R_c \sin(\alpha)} \cdot \mathrm{DW}(Q,\sigma) & \text{cylinders} \end{cases} \tag{4}$$

$\mathrm{DW}(Q,\sigma) = \exp(-Q^2{\sigma_{\mathrm{int}}}^2/2)$, where σ_{int} is the Gaussian width of the core−shell interface. R_c denotes the core radius, L the length of the cylinder, and α the angle between the cylinder axis and the scattering vector, $\mathbf{Q}$. $J_1(x)$ is the Bessel function of the first kind.

$$A(Q)_{sh} = \begin{cases} \dfrac{1}{C}\displaystyle\int_0^\infty 4\pi r^2 n(r) \frac{\sin(Qr)}{Qr}\, \mathrm{d}r\, DW(Q,\sigma) & \text{spheres} \\ \dfrac{1}{C}\displaystyle\int_{R_c}^\infty 2\pi r \cdot n(r) J_0(Q \cdot r \sin(\alpha))\, \mathrm{d}r\, DW(Q,\sigma) & \text{cylinders} \end{cases} \tag{5}$$

C is a normalization constant obtained by integration the density profile over the volume and J_0 is the Bessel function of the zeroth order. The density profile can conveniently be chosen to have the following generic form:

$$n(r) \sim \frac{1}{1 + \exp((r - R_m)/(\sigma_m R_m)} \tag{6}$$

where σ_m is the relative width of the micellar surface and R_m is the mean radius of the micelle. V_{PEP}, V_{PEO}, and $V_{PEP-PEO}$ are the molecular volumes of the PEP block, the PEO block and the overall PEP−PEO block copolymer (both block copolymers (hh and dd) have essentially identical volumes). $F(Q)$ is the effective scattering from the PEO polymers constituting the corona ("blob scattering"). The complete expressions for both the spherical and cylindrical case are given in ref 24.

The time dependence enters via the change of contrast of core and corona, $\Delta\rho_c^i(t)$, $\Delta\rho_{sh}^i(t)$ as a consequence of chain exchange between the differently labeled micelles. Even though after mixing and during the course of reaching a h-d equilibrium a strict distinction between the originally protonated and deuterated micelles gets lost, we can still write the contrast in terms of a surplus of either h or d chains $f(t)$ in the original h or d- type micelle. We will use the convention $f(t = 0) = 1$. Since the excess contrast is defined under zero average contrast conditions ($\rho_0 \approx (\rho_{hh} + \rho_{dd})/2$), $I(Q,t)^i$ must be symmetric around $f(t) \approx 0.5$, at least at low Q.[32] $f(t) \approx 0.5$ corresponds to the situation where the micelles are completely randomized.

The contrast for the h and d-cores at time t is then given by

$$\Delta\rho_c^i(t) = \begin{cases} \rho_{\mathrm{h-PEP}} \cdot f(t) + \rho_{\mathrm{d-PEP}} \cdot (1 - f(t)) - \rho_0 & \text{h-type micelle} \\ \rho_{\mathrm{h-PEP}} \cdot (1 - f(t)) + \rho_{\mathrm{d-PEP}} \cdot f(t) - \rho_0 & \text{d-type micelle} \end{cases} \tag{7}$$

and likewise for the corona

$$\Delta\rho_{sh}^i(t) = \begin{cases} \rho_{\mathrm{h-PEO}} \cdot f(t) + \rho_{\mathrm{d-PEO}} \cdot (1 - f(t)) - \rho_0 & \text{h-type micelle} \\ \rho_{\mathrm{h-PEO}} \cdot (1 - f(t)) + \rho_{\mathrm{d-PEO}} \cdot f(t) - \rho_0 & \text{d-type micelle} \end{cases} \tag{8}$$

where the excess function is restricted to the range: $0.5 \le f(t) \le 1$. As will clearly be verified in the subsequent section, the structure of the protonated and deuterated micelles are very similar and thus we can safely assume that $V_h^{\mathrm{mic}} \approx V_d^{\mathrm{mic}}$. Thus, the complete time dependent scattered intensity can be calculated by taking the average of the two "types" of micelles in the following way

$$I(Q,t) = \frac{1}{2}(I(Q,t)^{\mathrm{h}} + I(Q,t)^{\mathrm{d}}) + B \tag{9}$$

where $I(Q,t)^{h,d}$ is calculated according to eq 3 and B is a constant (time-independent) background reflecting the incoherent scattering of the sample. In analogy to the determination of $R(t)$ in eq 2 we can calculate $f_{\mathrm{exc}}(t)$ for a better comparison of the kinetic data obtained by the two methods:

$$f_{exc}(t) = \frac{f(t) - f_\infty}{f(0) - f_\infty} \tag{10}$$

3. RESULTS AND DISCUSSION

The structure and thermodynamics of the block copolymer micelles in different DMF/water mixtures were thoroughly investigated for the case of h-PEP1−h-PEO1 in a wide range of DMF/water solvent mixtures in a previous publication.[24] Nevertheless, since we are also dealing with the deuterated analogue, d-PEP1−d-PEO1, we will compare and discuss the overall structure of the micelles formed by the two block copolymers. The data are compared and analyzed for two selected DMF/water compositions, (X_{DMF} = 41% and 75%), where the block copolymers either form cylinders or spherical micelles. Subsequently, we will present the results for the exchange kinetics obtained for several DMF/water mixtures, (X_{DMF} = 41%, 47%, 51%, 60%, and 75%) by the time dependent small angle scattering experiment. Finally, we will discuss the observed kinetics for both spherical and cylindrical geometry in terms of the Halperin and Alexander scaling model taking into account the polydispersity of the core forming PEP-block. This will give further insight into the chain exchange mechanism in particular on the adopted chain conformation during the expulsion or insertion process.

3.1. Structure: SANS and Data Analysis. In Figure 2 scattering curves obtained for the two different block copolymers, h-PEP1−h-PEO1 and d-PEP1−d-PEO1 are shown for two DMF/water compositions of X_{DMF} = 0.41 and 0.75. The results were obtained under "full contrast conditions", i.e., by measuring

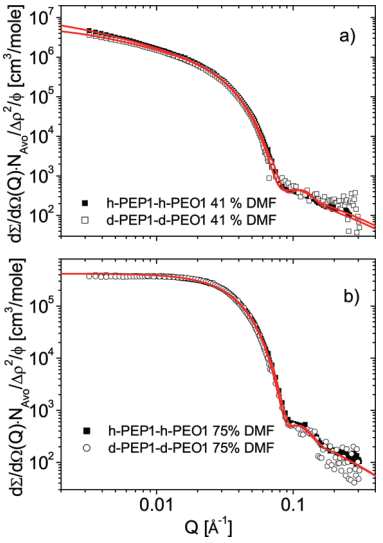

Figure 2. Normalized small-angle neutron scattering data of h-PEP1−h-PEO1 and d-PEP1−d-PEO1 in X_{DMF}= 41% and 75% under full contrast. The solid lines represent the best fit to a detailed core−shell scattering model for either (a) cylindrical or (b) spherical geometry. The data have been normalized with respect to the overall contrast and volume fraction for a better comparison.

the protonated block copolymer in fully deuterated solvent mixtures and vice versa for these selected samples.

We see that the at X_{DMF} = 0.41 both the hh and dd polymer form cylindrical structures while at X_{DMF} = 0.75 spherical micelles are obtained. This is consistent with a systematic structural study where we found that the PEP1−PEO1 system shows a transition between cylinders and spheres at around 50% DMF mol fraction in the solvent mixture.[24] As it was extensively discussed there, this is a consequence of the balance of the elastic energy associated with the chain stretching inside the micellar cores and the steric/elastic energy of the corona chains. While the former would favor cylindrical micelles since these exhibit the smallest radius for the same interfacial energy per chain,the corona free energy is higher in cylinders compared to spheres. Thus, as also shown with detailed thermodynamical calculations in ref 24, the balance is dictated by the interfacial tension which decreases with increasing DMF concentration. At high interfacial tensions, this allows the core size to decrease and thus the elastic core energy is negligible which consequently favors spherical micelles.

In the context of this paper it is important to verify that the micelles used for the kinetic investigation are similar. This is evident from the scattering data of the hh and dd micelles shown in Figure 2 which are within the error bars essentially the same. This is further confirmed by comparing the fit parameters compiled in Table 2. It is known from the polymer analysis that both polymers have very similar characteristics. Consequently, it can be concluded that there is no severe isotope effect in the aggregation behavior. It is further important to note that also under reduced contrast in the isotopic solvent mixtures used for the kinetic study the scattering curves are almost identical. This confirms that the calculated average scattering length density of the two polymers is always nicely matched by the used solvent compositions. A detailed structural characterization of micelles formed in X_{DMF} = 0.47 and X_{DMF} = 0.60 has not been performed in full contrast. Under zero average contrast conditions, however, the scattering curves of the hh and dd micelles are again exactly

Table 2. Micellar Characteristics of PEP1−PEO1 in two DMF/Water Compositions[a]

sample[b]	morph.[c]	R_c/Å	R_m/Å	R_g/Å	σ_{int}/Å
hh 41	C	43 ± 2	88 ± 9	15 ± 3	9 ± 3
dd 41	C	44 ± 2	85 ± 11	15 ± 2	10 ± 3
hh 75	S	44 ± 2	66.2 ± 6	14 ± 3	7.3 ± 3
dd 75	S	44 ± 3	61.5 ± 7	15 ± 2	5.6 ± 2

[a] Key: R_c, core radius; R_m, overall micellar radius; R_g, radius of gyration of PEO chains in the corona; σ_{int}, Gaussian smearing of the core−corona interface. In all cases the smearing coefficient characterizing the corona outer surface, σ_m, was set to 1%. [b] The numbers denote the DMF content in mol % [c] Morphology: cylinders (C) or spheres (S).

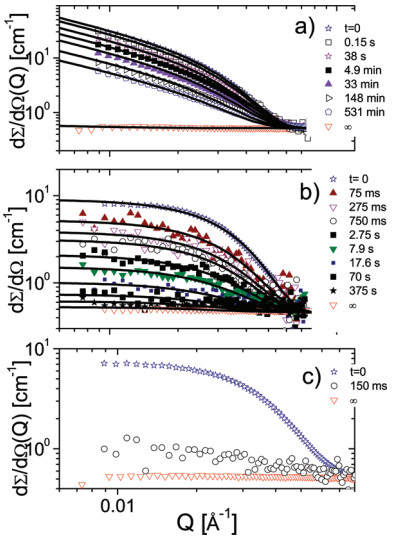

Figure 3. Small-angle neutron scattering data obtained by mixing deuterated and protonated micelles in a stopped-flow apparatus and following the scattered intensity as a function of time. The data corresponds to PEP1−PEO1 micelles in (a) 41%, (b), 60%, and (c) 75% DMF/water solvent mixture. The solid lines display fits to a time dependent core−shell scattering model. All data were recorded at 25 °C. The 41% and 75% data were obtained at the D11 instrument, while that of 60% DMF was measured at KWS2.

the same. Hence these two systems were also taken for studying the chain exchange kinetics by the time-resolved SANS method.

3.2. TR-SANS and Exchange Kinetics: Sensitivity to Interfacial Tension. The time dependence of the scattering curves in an intermediate Q-range after mixing the deuterated and protonated micelles in a zero-average contrast solvent is depicted for several DMF/water compositions in Figure 3.

As expected from previous work,[11] the time scale on which the kinetics occurs strongly depends on the DMF fraction in the selective solvent mixture. Measurements were not performed in pure water because previous experiments have shown that for PEP1−PEO20, which is much more hydrophilic than the present one, the micelles are completely frozen.[11] Still at 41% DMF, the kinetics is rather slow and occurs on a time scale of minutes-hours. However, upon increasing the DMF fraction up to 60% and 75%, the kinetics becomes much faster and is shifted to the subseconds−seconds range which makes it increasingly difficult to resolve even after using a stopped-flow apparatus for rapid mixing. In the case of 75% DMF the kinetics is practically

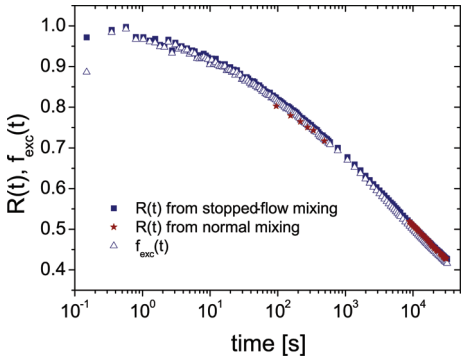

Figure 4. Comparison of kinetic data of PEP1−PEO1 in a water/DMF mixture with 41% DMF obtained by different methods: f_{exc} extracted from a full core/shell analysis, $R(t)$ evaluated from the integral intensity method and $R(t)$ using the manual mixing instead of the stopped flow technique.

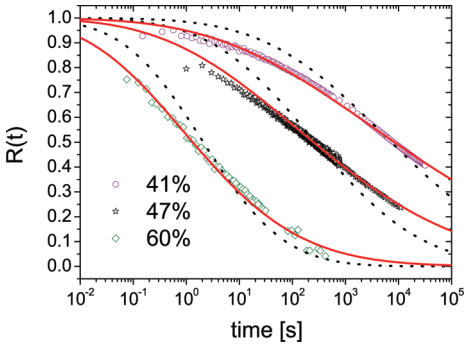

Figure 5. Relaxation function for the exchange kinetics, $R(t)$, for PEP1−PEO1 at three DMF/water compositions, 41, 47, and 60% DMF on a logarithmic time scale. Fits of theoretical model including the polydispersity of the PEP block are shown as dotted lines for $E_a \sim N_B^{2/3}$, and as solid lines for $E_a \sim N$ indicating a more stretched chain conformation of the PEP chain inside the PEO corona. The data corresponding to the 41% % was acquired at the D11 instrument, while that of 47% and 60% DMF was measured at KWS2.

unresolvable since it would require a time resolution below 75−150 ms which is currently not easily achieved with present reactor-based SANS instruments. The strong dependence on DMF composition can qualitatively be attributed to the interfacial tension which decreases strongly from 46 mN/m in pure water to about 8 mN/m in pure DMF. We will come back to this feature more in detail a bit later when the kinetics is analyzed in detail.

In order to evaluate the effect of the mixing method, measurements of the PEP1−PEO1 in 41% DMF system were performed at D11 using manual mixing with a micropipet and fast mixing in a stopped-flow apparatus. As is obvious upon an inspection of Figure 4, both methods give the same results at long times. At short times, however, the advantage of a stopped-flow apparatus is obvious, as a first measurement is already obtained after 100 ms whereas manual mixing would give a dead time of the order of a minute. Thus, by stopped flow mixing a more complete kinetic curve can be achieved.

The TR-SANS data were quantitatively evaluated using the methods described in 3.2. At first we have determined the relaxation function $R(t)$ defined in eq 2. As already described there $R(t)$ represents a direct measure of the amount of block copolymer that has exchanged at least once.[11] An example of this function determined for the PEP1−PEO1 in 41% DMF is given in Figure 4.

Additionally, we have evaluated the TR-SANS data by determining f_{exch} using the model dependent method introduced in 3.2. With this method the whole scattering profile of the core shell structure is calculated taking into account cross-terms between core and corona that might give nonlinear effects on the scattering, i.e. in addition to a simple shift, a real time dependent change in the scattering pattern. In order to evaluate this, we decided to calculate the full core−shell scattering cross section as a function of time by explicitly taking into account the time dependence of the contrast of both core and corona. In the fits, the micellar parameters were determined by fitting the model to the static data (t = 0, initial state) and these were later held fixed; i.e., we assume that no significant change in the structural properties occurs under mixing. This is justified by the very similar structure of the two block copolymers found in section 2. In the kinetic fits the only free parameter was thereby $f(t)$.

The results of the fits are plotted as solid lines in Figure.3. As seen the data are all very well described by the model indicating that the time dependence of the signal indeed can only be assigned to the loss in contrast. A fit to the data of the "blend" sample (completely randomized 50/50 protonated/deuterated sample prepared ex situ) gave $f(\infty) \approx 0.5$ which confirms the validity of the model evaluation and further the accuracy of sample preparation. In Figure 4, a comparison between f_{exc} and $R(t)$ is shown for the system PEP1−PEO1 in the solvent mixture with 41% DMF. Both quantities give almost the same results. This is the case also for the other PEP1−PEO1 systems with different DMF/water compositions. In the remaining part, however, we will focus the discussion on $R(t)$ as this quantity is model independent and, importantly, was shown to accurately describe the kinetics. As seen in Figure 4, the relaxation function $R(t)$ shows an extended time decay which follows an almost logarithmic dependence at longer times in agreement with earlier studies on a similar block copolymer system.[10,11] We will discuss this property in the subsequent section in terms of current theoretical models.

3.3. Mechanism for Chain Exchange: Influence of Morphology and Chain Conformations. In Figure 5 the relaxation functions, $R(t)$, are compared for PEP1−PEO1 in different DMF/water compositions on a logarithmic time scale.

The data show an extended decay that occurs over several orders of magnitude. At intermediate to long times a near logarithmic decay is observed which is clearly different to an exponential decay. As extensively discussed in refs.,[10−12,17] such a decay is related to the expulsion rate of the chain ("reaction limited" kinetics) since free chain diffusion is expected to occur on a much faster time scale (≈ micro/milliseconds). It was verified in earlier works[10,11,16] that we can also disregard fusion/fission at equilibrium conditions since the extended swollen corona prevents micelles to overlap due to unfavorable entropic interactions.

The kinetics is then determined by the expulsion rate constant, which should be independent of time, and we can write: $R(t) = \exp(-kt)$. From the Halperin and Alexander theory we expect a rate constant on the Boltzmann/Arrhenius form; $k = 1/\tau_0 \exp(-E_a/k_BT)$, where τ_0 is a characteristic time. In this model the activation energy is given by the product of the interfacial area and the interfacial tension γ of the single (collapsed) block B. In the original paper by Halperin and Alexander this was written as $E_a = \gamma \cdot N_B \cdot l_B^2$, with N_B the degree of polymerization of the insoluble block B and l_B the monomer length. However, as

recently recognized[17,16] this is only correct up to a prefactor (scaling law). In fact, assuming a completely collapsed perfectly spherical solvent-free globule, the activation energy should be written as $E_a = \gamma \cdot (36\pi)^{1/3} \cdot (V_0)^{2/3} \cdot N_B^{2/3}$, where V_0 is the monomer volume. Deviation from this conformation would give different prefactors, and importantly, a different N_B dependence. In order to take this into account, we write the following for the rate constant:

$$k(N_B) = 1/\tau_0 \exp(-\alpha \cdot \gamma \cdot (36\pi)^{1/3} (V_0)^{2/3} N_B^{\beta}/k_B T) \quad (11)$$

where β is a scaling exponent which is $^2/_3$ for spherical globules and 1 for solvent surrounded linear chains. Thus, we would expect an exponent that has the following validity range: $^2/_3 \leq \beta \leq 1$. α is a prefactor that, together with β would correct for deviations from a spherical shape and/or interpenetration of solvent. For a completely stretched chain we can estimate a factor $(8\pi)^{1/3}$ instead of $(36\pi)^{1/3}$ in eq 11. Hence in this corresponding to $\beta = 1$, we would expect $\alpha \approx 0.6$.

As for the time scale, we follow the suggestion by Choi, Lodge and Bates[16] and choose the Rouse time as characteristic time: $\tau_0 = \tau_R = \xi N_B^2 l_B^2/(6\pi^2 k_B T)$. Here the effective segment length of PEP varies with temperature, which using data reported in the literature[35] takes the value of $l_B \approx 6.9 \exp(18/(T - 208)) = 8.4$ Å at 25 °C. The monomeric friction for PEP can likewise be calculated as: $\xi = 5.06 \times 10^{-13} \exp(490/(T - 260)) = 2.0 \times 10^{-7}$ Ns/m. The final expression for describing the kinetic data is then given by the average over the PEP block length distribution in the way we have proposed before[10,11] and later adapted by Choi et al.:[16]

$$R(t) = \int_1^{\infty} f(N_B, \sigma) \exp(-k(N_B)t)\, dN_B \quad (12)$$

Here $f(N_B)$ is the distribution function. Polymers prepared by living anionic polymerization exhibit a Poisson type chain length distribution. Since this distribution corresponds to a ideal theoretical situation where the polymerization has occurred without any side reactions and to 100% completion, we considered a two-parameter Schulz−Zimm distribution function which was used by Choi et al.[16] where the width and mean value can be adjusted independently to any given experimental situation:

$$f(N_B, \zeta) = \frac{\zeta^{\zeta+1}}{\Gamma(\zeta+1)} \cdot \frac{N^{\zeta-1}}{\langle N_B \rangle^{\zeta}} \exp(-\zeta \cdot N_B/\langle N_B \rangle) \quad (13)$$

Here $\zeta = 1/(M_w/M_n - 1)$, where M_w/M_n defines the polydispersity of the polymer. The values for the PEP blocks are given in Table 1. The results of the fits using eqs 11− 13 are depicted in Figure 5. In all fits using the Schulz-distribution, the sample-specific parameters were held fixed ($\langle N_B \rangle$ =17, M_w/M_n = 1.07 and the values for the interfacial tension of PEP in DMF/water were taken from earlier published data measured by the pendant drop method.[18]

First, the model (12) was fitted simultaneously to the three data sets using $\beta = ^2/_3$ and α as the only free parameter. This gave a very poor fit and consequently α was let to vary between the different data sets while all other parameters were held fixed. The best fit (smallest χ^2 value) was obtained using α = 0.56, 0.51, and 0.41 for the 41, 47, and 60% DMF/water solutions, respectively. These fits are shown for the Schulz-distribution as dotted lines in Figure 5. As seen the obtained agreement with the data is still very poor. It should be mentioned that much better agreement could be obtained using a M_w/M_n of about 1.15−1.16 but that can clearly be discarded from the polymer characterization where both the SEC and NMR results show that such polydispersities are impossible (see Table 1 and Figure 1). Consequently, the dependence of chain-length was modified by letting β as a free parameter. Here, as shown in Figure 5 as solid lines, a good fit was obtained with $\beta = 1$ (i.e., $E_a \sim N_B$). This gave $\alpha = 0.21 \pm 0.02$, 0.19 ± 0.02, and 0.15 ± 0.02 from the lowest to the highest DMF concentration. We will now discuss these fit results with respect to the exchange mechanism and its dependence on morphology. We will first focus on the value of α which controls the activation energy.

In all cases α is lower than one would expect from the estimates. Comparing to the value that would be expected for a fully stretched chain during the expulsion process (corresponding to $E_a \sim N_B$), we estimate that $\alpha \approx 0.6$. I.e. α is further reduced by at least a factor of 3. In addition a weak decrease of the parameter α is observed in parallel to the transition from cylinders to spheres. The statistical error for α obtained from fitting is small, of the order of less than 1%. It should however be mentioned that the fits are extremely sensitive to these values and experimental uncertainties arising, e.g., from polymer characterization, or interfacial tension measurements might be additionally present.

In order to further check whether the exchange kinetics really depends on morphology we further designed the following experiment. As shown in a previous paper,[24] the system undergoes a thermally induced irreversible cylinder-to-sphere transition in a 51% DMF composition. We thus performed a TR-SANS experiment at D11, ILL on exactly the same micellar solution before and after heating the sample at 70 °C for several hours. In this case the kinetics in cylindrical (prepared at room temperature) and spherical (heated) micelles could be compared directly and even subtle changes can be discerned.

The results after extracting $R(t)$ are compared in Figure 6. The data were obtained by averaging over five mixing runs. In order to demonstrate the excellent reproducibility results of two measurements (each averaged over five mixing runs to gain statistics) for one sample (heated 51% sample) are shown in the inset.

As seen there is a small but clear difference between the exchange kinetics in cylindrical and spherical micelles which is more visible at longer times. Apparently, chain exchange in the spherical micelles is slightly faster. Although this change is quite small we note that the difference is unambiguous and is not a result experimental uncertainties. This can be verified by comparing the data in the inset plot of Figure 6 which shows an excellent reproducibility of the kinetic results. In order to further analyze this difference in a more quantitative manner, we fitted the model described above to both sets of data using eq 12). The fits are shown as solid lines in Figure 6. The best description was obtained using a polydispersity index of 1.07 and α of 0.20 and 0.19 for the cylindrical and spherical micelles, respectively. The interfacial tension was set to 14.5 mN/m as determined earlier from interfacial tension measurements[18] while the polymer characteristics were fixed to the values listed in Table 1 as before.

As seen, the difference between the data sets can be condensed to a small decrease in α for the spherical micelles. This is in good accordance with the more pronounced decrease observed by varying the DMF concentration. It is therefore reasonable to assume an intrinsic effect which may originate from the following causes.

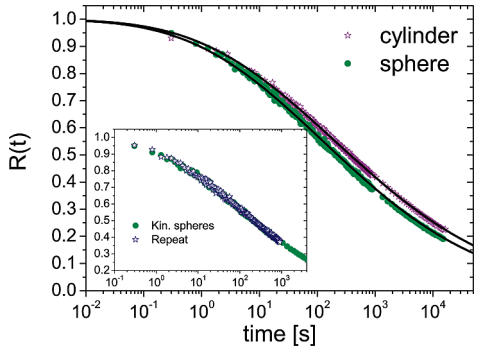

Figure 6. Relaxation function, $R(t)$, for the exchange kinetics of either cylindrical or spherical micelles formed by PEP1−PEO1 in 51% DMF solution. The data has been obtained by mixing hh and dd type micelles before and after thermally induced cylinder-to-sphere morphological transition. The inset shows the results from two separate measurements of the exchange kinetics in the spherical micellar state to show the reproducibility.

First, one needs to consider the enthalpic penalty of the expulsion process which in this model is essentially contained in $E_a \sim \alpha \cdot \gamma \cdot N_B$. Since γ is taken as the macroscopic value for a bare PEP/solvent interface, α might be thought of as a correction factor reflecting a different "microscopic" interfacial tension. However, this does not explain why the value for α varies for the different micellar morphologies. If we now take into account the concentration of the PEO block in the corona surrounding the micellar core, it becomes clear that the barrier for the expulsion process is modified by segmental contacts with PEO. These are determined by the density profile around the micelles which varies for different micelles and in particular for different micellar morphologies. To account for this, a first simplistic approximation would be to assume that the effective interaction parameter, directly related to the interfacial tension ($\gamma^2 \sim \chi$), follows a linear relationship: $\chi_{\text{eff}} = \Phi_{\text{PEO}} \cdot \chi_{\text{PEP/PEO}} + (1 - \Phi_{\text{PEO}}) \cdot \chi_{\text{PEP/solv}}$, with Φ_{PEO} the mean PEO concentration in the corona. Using this approach and inserting data obtained from the structural characterizations,[34] we obtain a reduction of γ of −5% for the cylinders in the 41% solution and −7% decrease for the 60% solutions with spherical micelles. Although this is a small difference the trend is in line with the observed extremely weak reduction of the parameter α which changes from 0.2 to 0.19 for the cylindrical and spherical micelles in 51% DMF/water solution. However, such decrease is too weak to claim that the presence of PEO corona chains significantly facilitates chain exchange *thermodynamically* by reducing the enthalpic cost in this particular micellar system.

In this context it is interesting to compare the results with data published on the self-diffusion in a series of poly(ethylene-*alt*-propylene)−poly(dimethylsiloxane) (PEP−PDMS) spherical block copolymer melts where α was found to vary substantially (0.27−1.34) between the various molecular weights/compositions.[36] Since α was found to increase with the degree of segregation, it was speculated that α directly reflects the density profile of the core−corona interface. In the case of a broad interface, a higher fraction of core chains will be already in contact with the solvent thus reducing the enthalpic barrier and hence decreasing α. A reduction of α was also found in the work of Choi et al.[16] in the case of PS−PEP in squalane. This system is weakly segregated with relatively low χ values[22] which would thus support such an "ansatz". For the present system, although characterized by rather large χ values, one would also expect a certain decrease in segregation as γ decreases with DMF concentration. This should be reflected in the width of the core−corona interface (σ_{int}) which from the fits is found to be larger for the cylindrical micelles than for the spherical ones. Thus, no direct support of such ideas can be found, although we note that such level of detailed structural information is extremely sensitive to subtle variations in background corrections etc.

As an alternative explanation, we have considered kinetic effects that also arise from changes in the polymer concentration in the corona surrounding the core. It was speculated that these effects dynamically retard the kinetics by obstruction or steric effects similar to the concentration dependence for self-diffusion in semidilute polymer solutions (see, e.g., ref 37). However this should not affect the activation energy and hence α but rather the time constant, τ_0. This was also considered by Halperin and Alexander who showed that the prexponential factor depends on micellar type; they considered star-like micelles and crew cut micelles, respectively. For the latter type they predicted $\tau_0 \sim N_B^{7/3}$ which is only marginally different to the N_B^2 dependence considered here. We will therefore not further discuss different N_B dependencies. Instead fits were performed now modifying the Rouse time constant according to $\tau_0 = \tau_R \times$ const and keeping α constant. However, we could not obtain reasonable fits and this approach was discarded.

Halperin and Alexander in their original paper, did not consider the possibility that the activation energy term varies with micellar structure. However it is possible to imagine that crowding and high polymer density can affect the conformation of the expelled chain. Hence for dense systems where the typical radius of gyration is smaller than the blob size of the corona, the chain is likely to stretch out in order to escape the dense polymer network. This would affect the activation energy and thus provides an explanation of the stretched conformation associated with the found linear dependence between the activation energy and the number of monomers, i.e. the $E_a \sim N_B$. Instead, if the polymer collapses directly on the interface, one would expect $E_a \sim N_B^{2/3}$. The two different physical pictures are given in Figure 7.

The fit results show that, irrespective of the value for α and independent of the morphology, a good description is obtained using $\beta = 1$. This indicates that the insoluble PEP block preferably assumes a stretched conformation during the expulsion process which involves the diffusion out from the core, through the corona into the solution. This might be a consequence of the rather short PEP chains in the present case which inhibits a statistically favorable formation of a compact globule. This would be in complete analogy with surfactant micelles which would be expected to follow the same scaling. However, such a linear dependence, $E_a \sim \chi N_B$, was also obtained by Choi, Lodge, and Bates where the investigated system with large number of core block repeat units of the order of 200−400 in a system of PS−PEP micelles in squalane. The present results should also be compared with earlier studies on an asymmetric block copolymer, PEP1−PEO20, which forms starlike micelles in water/DMF mixtures. Here the results obtained by a simultaneous fit of data at different temperatures indicated that a $E_a \sim N_B^{2/3}$ law could describe the data rather satisfactorily. It should be pointed out that these results were obtained using the manual mixing method and thus lacks the initial decay curve. Nevertheless, the results imply the compact globular conformation. We could try to explain this observation by the fact that the

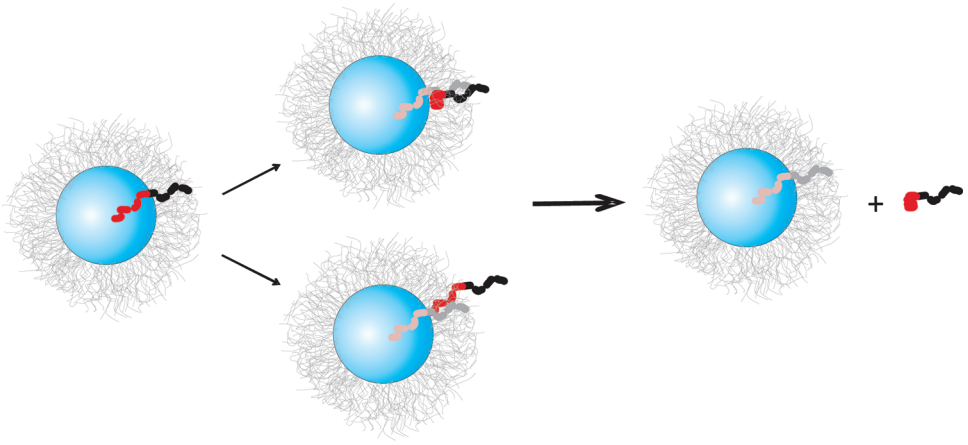

Figure 7. Schematic illustration of the expulsion process. The two limiting situations characterizing a stretched (lower middle) and compact (upper middle) conformation during the expulsion process is shown. The former would have a stronger dependence on the core chain length than the latter; $E_a \sim N_B$ and $E_a \sim N_B^{2/3}$, respectively, as discussed in more detail in the text.

"star-like" micelles have quite dilute coronas (more than a factor 5 less than here) and that the chain could escape more freely through the corona.

To elaborate this hypothesis further, we should calculate the smallest blob size of the corona, ξ_{min} which is approximately given by $\xi_{min} \approx (s_0)^{1/2}$. Here s_0 is the area per chain at the interface given by $s_0 = 2\pi R_c \cdot L/P$ and $s_0 = 4\pi R_c^2/P$, for cylindrical and spherical geometry, respectively. Inserting the numbers given in ref 24, we see that for the PEP1−PEO1 micelles the number ξ_{min} increases from about 10−11 Å for the cylinders to about 13 Å for the spherical micelles upon increasing the DMF content. For spherical and cylindrical micelles in 51% DMF the values obtained earlier is about 12 and 13 Å respectively. This should be compared with the radius of gyration of the PEP block; $R_g \approx$ 14 Å. Hence, for the current system ξ_{min} is slightly smaller than R_g. For the star-like PEP1−PEO20 micelles,[18] however, we obtain values in the range of 14−16 Å, which thus is larger. This could thus support the idea of a more restricted motion of the PEP chain through the "crew-cut" PEP1−PEO1 micelles as compared to the PEP1−PEO20 "star-like" micelles. It is interesting to here also compare the current system with the PS−PEP micelles investigated by Bates et al.[16] On the basis of the structural data given in ref 16 ($P \approx 69$; $R_c \approx 88$ Å), we estimate a $\xi_{min} \approx 37-28$ Å, which is considerably smaller than the estimated R_g of about 108 Å for a 26 600 g/mol chain.[38] Hence in this case it is even more likely that the PS chain needs to stretch to an even greater extent in order to escape through the corona and out of the micelle. However, it should be mentioned that the PS−PEP/squalene system is expected to be very close to a Θ-system[22] and thus one might argue that a $E_a \sim N_B$ law is here expected a priori.

In any case, this discussion remains a hypothesis and further experimental and theoretical work is required in order to verify the effect of corona structure on the exchange mechanism.

Finally, it should be mentioned that while this paper was in the review process, two further articles on this topic appeared concerning exchange kinetics at higher concentration.[39,40] In the work by Choi et al.,[39] its was experimentally shown that the exchange kinetics occurs more slowly in the ordered state compared with that in dilute solutions which could be summarized in a 10% increase in the effective activation energy ($\alpha \cdot \chi$). It was speculated that this was due to either a change in the core (glass transition) or micellar structure (density profile). In the theoretical paper by Halperin,[40] the slowing down of the exchange kinetics was attributed to an increased osmotic pressure associated with increased coronal chain overlap that leads to an increased penalty for exchange kinetics. Although this corresponds to a different situation compared to ours, it shows that the internal micellar structure indeed plays a role in the exchange kinetics.

4. CONCLUSION

In this work, we have systematically investigated the exchange kinetics in block copolymer micelles across the cylinder-to-sphere transition by millisecond TR-SANS using a sophisticated contrast variation technique and detailed model fitting. Upon comparing results from cylindrical and spherical micelles in exactly the same solution and total concentration, we can conclude that there is slight but clearly measurable increase in the exchange kinetics of the spherical micelles.

The results show that the kinetics can be described by a model for chain expulsion limited kinetics including the finite polydispersity of the polymer system, independent of the morphology. This model was originally developed in refs 10 and 11 and later modified by Choi et al.[16] to include the Rouse time, τ_R, as the prexponential factor setting the time scale and by allowing a free scaling parameter, α, for the activation energy.[24] The subtle dependence of the morphology on the exchange kinetics can be summarized in a slightly smaller α parameter for the spherical micelles.

In the previous work on star-like micelles in refs 10, 11, and 24, it was found that the activation energy scales like $E_A \sim N_B^{2/3}$, while for the present cylindrical and spherical crew-cut micelles we find a stronger chain length dependence of the activation energy, $E_A \sim N_B$. We speculate that this is caused by the adopted conformation of the core chains which need to be stretched in order to facilitate the passage through the dense corona. The previously studied star-like block copolymer micelles on the other hand consist of much more dilute coronas which exhibit less constraints on the chain conformation during the diffusion process.

The fits were performed essentially with only one free parameter, α that matches the activation energy as $E_a \sim \alpha \cdot \gamma \cdot N_B$. All

other parameters are known from the polymer characterization, including the interfacial tension, γ. In the analysis, we found that α decreases upon changing the morphology from cylindrical to spherical micelles. It is possible that the found small variances reflect subtle structural features such as the density profile over the core−corona interface, and/or corona structure and that these local structural factors are slightly dependent on the morphology. However, to verify this, further experimental results of different block copolymer micellar systems would be needed. In particular a combination of both very detailed structural characterizations and kinetic analysis is important to delineate such effects.

AUTHOR INFORMATION

Corresponding Author

*E-mail: (R.L.) reidar_lund@ehu.es; (L.W.) l.willner@fz-juelich.de.

ACKNOWLEDGMENT

The authors acknowledge support of the European Community within the SoftComp Network of Excellence (NoE) program. R.L. and J.C. also acknowledge support from the following grants: GIC07/35-IT-463-07, MAT2007-63681, and CSD2006-00053.

REFERENCES

(1) Tuzar, Z.; Kratochvil, P. *Adv. Colloid Interface Sci.* **1976**, *6*, 201.
(2) Hamley, I. W. *The Physics of Block Copolymers*; Oxford University Press: Oxford, U.K., 1998.
(3) Wennerström, H.; Lindman, B. *Phys. Rep* **1979**, *52* (1), 1.
(4) Aniansson, E. A. G.; Wall, S. N. *J. Chem. Phys.* **1974**, *78* (10), 1024.
(5) Aniansson, E. A. G.; Wall, S. N. *J. Chem. Phys.* **1975**, *79* (8), 857.
(6) Aniansson, E. A. G.; Wall, S. N.; Almgren, M.; Hoffmann, H.; Kielmann; Ulbricht, W.; Zana, R.; Lang, J.; Tondre, C. *J. Phys. Chem.* **1976**, *80*, 905.
(7) Halperin, A. *Europhys. Lett.* **1989**, *8*, 351.
(8) Halperin, A.; Alexander, S. *Macromolecules* **1989**, *22*, 2403.
(9) Willner, L.; Poppe, A.; Allgaier, J.; Monkenbusch, M.; Richter, D. *Europhys. Lett.* **2001**, *55* (5), 667.
(10) Lund, R.; Willner, L.; Stellbrink, J.; Lindner, P.; Richter, D. *Phys. Rev. Lett.* **2006**, *96*, 068302.
(11) Lund, R.; Willner, L.; Dormidontova, E. E.; Richter, D. *Macromolecules* **2006**, *39*, 4566.
(12) Lund, R.; Willner, L.; Richter, D.; Iatrou, H.; Hadjichristidis, N.; Lindner, P. *J. Appl. Crystallogr.* **2007**, *40*, s327.
(13) Procházka, K.; Bednář, B.; Mukhtar, E.; Svoboda, P.; Trněná *J. Phys. Chem.* **1991**, *95*, 4563.
(14) Wang, Y.; Kausch, C. M.; Chun, M.; Quirk, R. P.; Mattice, W. L. *Macromolecules* **1995**, *28*, 904.
(15) Waton, G.; Michels, B.; Zana, R. *Macromolecules* **2001**, *34*, 907.
(16) Choi, S. O.; Lodge, T. P.; Bates, F. S. *Phys. Rev. Lett.* **2010**, *104*, 047802.
(17) Lund, R.; Willner, L.; Stellbrink, J.; Lindner, P.; Richter, D. *Phys. Rev. Lett.* **2010**, *104*, 049902(E).
(18) Lund, R.; Willner, L.; Stellbrink, J.; Radulescu, A.; Richter, D. *Macromolecules* **2004**, *37*, 9984.
(19) Krutyeva, M.; Martin, J.; Arbe, A.; Colmenero, J.; Mijangos, C.; Schneider, G. J.; Unruh, T.; Su, Y.; Richter, D. *J. Chem. Phys.* **2009**, *131*, 174901.
(20) Martin, J.; Krutyeva, M.; Monkenbusch, M.; Arbe, A.; Allgaier, J.; Radulescu, A.; Falus, P.; Maiz, J.; Mijangos, C.; Colmenero, J.; Richter, D. *Phys. Rev. Lett.* **2010**, *104*, 197801.
(21) Willner, L.; Lund, R.; Monkenbusch, M.; Holderer, O.; Colmenero, J.; Richter, D. *Soft Matter* **2010**, *6*, 1559.
(22) Lund, R.; Willner, L.; Alegria, A.; Colmenero, J.; Richter, D. *Macromolecules* **2008**, *41*, 511.
(23) Fatkullin, N.; Kimmich, R.; Fischer, E.; Mattea, C.; Beginn, U.; Kroutieva, M. *New J. Physics* **2004**, *6*, 46.
(24) Lund, R.; Pipich, V.; Willner, L.; Radulescu, A.; Colmenero, J.; Richter, D. *Soft Matter* **2011**, *7*, 1491.
(25) Allgaier, J.; Poppe, A.; Willner, L.; Richter, D. *Macromolecules* **1997**, *30* (6), 1582.
(26) Lindner, P. Scattering experiments: experimental aspects, initial data reduction & absolute calibration. In *Neutrons, X-Rays and Light: Scattering methods applied to soft condensed matter*; Lindner, P., Zemb, Th., Eds.; Elsevier−North Holland Delta Series: Amsterdam, 2002.
(27) Pedersen, J. S.; Svaneborg, C. *Curr. Opin. Colloid Interface Sci.* **2002**, *7*, 158.
(28) Pedersen, J. S.; Posselt, D.; Mortensen, K. *J. Appl. Crystallogr.* **1990**, *23*, 321.
(29) QtiKws was developed by Dr. Vitaliy Pipich at JCNS, Garching, Germany.
(30) Smith, G. D.; Yoon, D. Y.; Jaffa, R. L.; Colby, R. H.; Krishnamoorti; Fetters, L. J. *Macromolecules* **1996**, *29*, 7602.
(31) Sommer, C.; Pedersen, J. S.; Stein, P. C. *J. Phys. Chem.* **2004**, *108*, 6242.
(32) This is only valid considering an *average value* at low Q where at average the micelles can be regarded as effectively homogeneous on the length scales probed. On higher Q-values there might be excess scattering arising from inhomgeneties in composition *within* the micellar core etc. Nevertheless, the goodness of the fits up to relatively high Q seems to indicate that this is not a significant effect.
(33) Poppe, A., Ph.D Thesis, University of Münster: Germany, 1999.
(34) From the literature,[33] we can estimate the interaction parameter between PEP and PEO to be about 0.5 while the values for PEP with respect to the solvent molecules we can estimate from the interfacial tension via the Helfand equation ($\gamma = k_B T/l_0^2(\chi_{PEP-solv}/6)^{1/2}$). Using a unit length scale of l_0 = 5 Å we obtain χ-values of 6 and 3 for interfacial tensions corresponding to 41 and 60% DMF respectively. Hence polymer contacts between PEP and PEO are favoured over PEP and solvent. The mean PEO concentration in the corona, $\Phi_{PEO} = P \cdot V_{PEO}/((4/3)\pi(R_m^3 - R_c^3))$, was calculated to be between 25 and 30. With respect to $\chi_{PEP/solv}$ the effective χ-parameter, χ_{eff}, is 23% lower for the cylindrical micelles in 41% DMF and 26% lower for the spherical micelles in 60% DMF respectively. This corresponds to a relative *decrease* of the effective χ-parameter of the order of 23% for the cylindrical and 26% for the spherical micelles respectively and translates to a 5% and 7% decrease in terms of γ.
(35) Richter, D.; Monkenbusch, M.; Arbe, A.; Colmenero, J. *Nesutron Spin Echo in Polymer Systems*; Advances in Polymer Science 173, Springer: Berlin, Germany, 2005.
(36) Cavicchi, K. A.; Lodge, T. P. *Macromolecules* **2003**, *36*, 7158.
(37) Zettl, U.; Hoffmann, S. T.; Koberling, F.; Krausch, G.; Enderlein, J.; Harnau, L.; Ballauf, M. *Macromolecules* **2009**, *42*, 9537.
(38) Fetters, L. J. In *Physical Properties of Polymers Handbook*, 2nd ed.; Mark, J. E., Ed.; Oxford University Press: New York, 2009.
(39) Choi, S. O.; Bates, F. S.; Lodge, T. P. *Macromolecules* **2011**, *44*, 3594.
(40) Halperin, A. *Macromolecules* **2011**, *44*, 5072–5074.